NON LINEAR ANALYSIS OF SHEAR DEFORMABLE ANISOTROPIC PLATES

Erasmo CARRERA

DIAS, Politecnico di Torino,

Corso Duca degli Abruzzi,.24, 10129 Torino, Italia

Abstract

This paper deals with the nonlinear static analysis of multilayered elastic plates subjected to conservative loads. Based on Reissner-Mindlin theory FSDT (First Shear Deformation Theory) a finite element model is developed. Nonlinearities of von Kármán type are taken into account. A four node plate finite element with assumed shear strain fields is employed in the numerical investigations. For purpose of comparison the results related to the classical Kirchhoff plate approximations CLT (Classical Lamination Theory) are obtained by application of a penalty technique to the shear correction factor. Numerical studies concern the postbuckling behaviour of plates accounting several geometries (square and rectangular, thick and thin plates), laminations (symmetrical and not symmetrical), loading cases (axial and biaxial compression, shear and combined loadings) and geometrical boundary conditions (simply supported, hinged and clamped edges). The following main conclusions have been acquired. 1) The FEM is a good tool to trace the postbuckling of anisotropic flat panels. Further in respect to other approximate methods, its possible application does not depend on both boundary conditions and lamination schemes. 2) It is confirmed that the nonlinear effects are very important in the analysis of multilayered plates and that the shear deformation effects are very much subordinate to both multilayered lay-up and loading configuration, furthermore they are greater in the large deflections field. 3) In respect to prebuckling and buckling analyses, much more care should be taken to impose boundary conditions when the postbuckling range has to be traced.

1 Introduction

Composite technology has played and will continue to play an important role in the aerospace industry. Taking advantage of their light weight, high strengh and anisotropic properties, which can be tailored by varying the fiber orientation and stacking sequence, laminated composites can be used to fabricate highly efficient structures. While these material possess all the above advantages, their structural response is quite complicated and still not fully understood. One of the important problems deserving special attention is the study of their nonlinear response in both sense of large deflections and postbuckling. In fact the well-known postbuckling strength exhibited by metallic panels has permitted the design of conventional aircraft structural elements to operate within the postbuckling range and evidently a better understanding of the postbuckling behaviour of composite panels constitutes an essential requirement toward a rational employment of their strength. Experimental research activities are carried out in many laboratories over the world; see Chai, Banks and Rhodes [1] as a recent example and for literature. Usually these are very expensive and the cost of a parametric study becomes prohibitive. From this point of view attempts to model analytically and numerically the nonlinear behaviour of composite structures are very welcome. To this argument the attention of the present paper is devoted. Some aspects which are useful for our purpose are discussed in the following text.

The first one coming from the last twentyfive years literature concerns the two-dimensional theories for modelling anisotropic structures. Considerable literature (among the others see the review article of Noor and Burton [2]) has shown that increasing the orthotropic ratio of the lamina and the plate thickness, the transverse shear deformation effects cannot be neglected and the classical Kirchhoff plate approximations CLT (Classical Lamination Theory) must be substituted at least by Reissner-Mindlin model, FSDT (First Shear Deformation Theory). To notice that many improved theories, including Higher-order effects HSDT (Higher order Shear Deformation Theory), are available from the open literature, especially in order to characterize local phenomena; these will not be considered in the present work. Furthermore the articles by Librescu and Stein [3], by Librescu and Chang [4], [5], by Palazotto and Tsai [6] and by Carrera and Villani [7] have shown that the shear deformation could assume even more importance in the large deflections range.

Another important aspect concerns not symmetrically laminated plates (in respect to their middle plane). The coupling between in-plane and out of plane strains exhibited by such plates makes the effects of nonlinear terms very important even though low level of the in-plane applied loads are considered, see Sun and Chin [8] and Jensen and Lagace [9]. For such plates the classical buckling load of Euler-type analysis looses sense, as well discussed by Leissa in [10]. Moreover dealing with the cylindrical bending of asymmetrically laminated plates, the author in [11] has found the possibility of a snapping-type phenomenon for the compression loading case, i.e. the nonlinear terms have tragic effects.

Although many papers and results are available for the linear analysis including FSDT and HSDT effects, the literature is quite exiguous about nonlinear response of generally laminated composite plates. These results are even less when shear deformable and/or not symmetrically laminated plates are considered. That is mainly due to the following reasons: (1) analytical closed form solutions are available only for very few cases related to simple lamination sequence, geometries and boundary conditions; (2) when approximated methods are employed the computational costs of a nonlinear analysis are very high mainly because a system of nonlinear equations must be solved iteratively at each loadstep. Applications to the large deflections analyses of analytical methods as those quoted in Chia's book [12], in the already mentioned papers [3],[4],[5] and in those cited in the overview article by Chia [13], are quite attractive. Their limitations hold upon the fact that the possibility of finding an approximate solution is strongly dependent on both boundary conditions and multilayered lay-up, in fact to these must be related the shapes employed in the *a priori* expansions of the unknown functions. Within these subjects very welcome are the recent progresses made by approximated methods of the computational mechanics and particularly by the FEM (Finite Element Method), as tools to trace the nonlinear response of many different problems: see [14] for isotropic structures and [15] for multilayered ones. In fact by the use of FEM techniques the limitations of the analytical methods are easily subjugated, nevertheless FEM formulations (especially when concern plates and shells) are very often affected by numerical deficiencies as locking which can be overcome by implementation of some numerical tricks, see [16].

The present work is a sequel of previous author's works [7], [11],[17] and [18] directed to investigate composite plates by FEM. It uses a shear deformable plate finite element of Reissner-Mindlin type. Nonlinearities of von Kármán type are included (large rotations, large strains and material nonlinearities are not considered herein). To the end to obtain low band length of FEM stiffnesses matrixes the simple four node plate element $Q4$ is imployed. The numerical efficiency of this element has

been reached by application of assumed shear strain fields concept discussed by Dvorkin and Bathe [19] and Hinton and Huang [16] among the others. The multilayered formulation of this element has been proposed by the author in [20] and implemented in the FEM code MATCO which is available at DIAS. For purpose of comparison the CLT results are obtained by implementation of a penalty technique applied to the shear correction factor. Elastic flat plates subjected to static conservative loads are considered. Both symmetrically and not symmetrically anisotropic laminated plates are analyzed. As novelty in respect to the previous works, compression (in both directions), in-plane shear and combined loading cases are investigeted. Furthermore new boundary conditions and plate geometries are explored. The contents have been organized as follow. Sec.2 quotes outlines of the governing FEM equations, describing the standard solution methods of the nonlinear system of algebraic equations and the used Reissner-Mindlin finite plate multilayered elements; numerical investigations are performed in Sec.3 to which the concluding remarks follow.
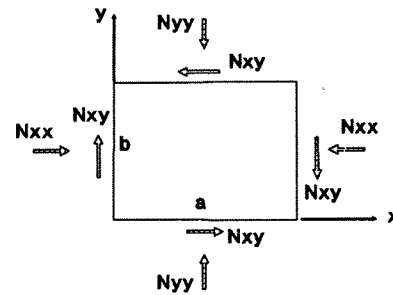

Figure 1: Plate geometry and notations.

2 Outlines of FEM descriptions

2.1 Governing equations

Consider an elastic body subjected to static loads and under prescribed boundary conditions. If the body is assumed to execute an arbitrary set of infinitesimal virtual displacements, from the actual configuration, the following variational equation holds [21]

$$\delta\Psi = \delta W \qquad (1)$$

$\delta\Psi$ is the virtual variation of the strain energy and δW is the virtual variation of the external work. Upon application of FEM approximations, the variational equation (1) then reduces to a nonlinear set of algebraic equations that we write in the two following equivalent forms [22], [23]

$$\{\varphi(\{q\}, \{p\})\} = 0; \quad [K_s(\{q\})]\{q\} = \{p\} \qquad (2)$$

where[1]:

{q} is the n-dimensional vector of the nodal displacements and/or rotations;

{φ} is the n-dimensional vector of the resultant nodal forces (inner plus external forces);

{p} is the n-dimensional vector of the nodal forces equivalent to the external loads (which is assumed deformation independent);

$[K_S]$ is the secant stiffness matrix.

The Eqn.(2) constitutes the point of departure for finite element calculation of geometrically nonlinear systems. In addition it's assumed that the structure is subjected to a proportional loading

$$\{p\} = \lambda\{f\} \tag{3}$$

where {f} denotes a fixed reference load vector and λ is a load-scaling factor, *load parameter*.

2.2 Standard solution method

The Eqn.(2) gives the FEM model of the physical problem. A standard solution scheme is obtained through the following straightforward application of the Newton's method between the initial state i and the unknown state $i+1$ (in the neighbourhood of i):

$$\{\varphi_{res}\} = [\{\varphi\}_{,\{q\}}]\{\Delta q\} + [\{\varphi\}_{,\{p\}}]\{\Delta p\} \tag{4}$$

in which the load level is treated as a variable; the notation $,_.$ denotes partial derivative. Within the limits of our assumptions we have

$$\{\Delta p\} = \Delta\lambda\{f\}; \quad \{\varphi_{,\{q\}}\} = [K_T(\{q^i\})]$$
$$\{\varphi_{,\{p\}}\} = -[I] \tag{5}$$

where

$[K_T]$ is the tangent stiffness matrix;

$[I]$ is the unit matrix;

$\{\Delta q\} = \{q^{i+1}\} - \{q^i\}$ is the incremental nodal displacement vector;

$\Delta\lambda = \lambda^{i+1} - \lambda^i$ is the incremental load factor;

$\{\varphi_{res}\} = [K_s\{q^i\}]\{q^i\} - \lambda^i\{f\}$ is the residual nodal vector of the nodal forces (unbalanced nodal forces vector).

---

[1]Brace and square brackets denote vectors and matrices respectively. We refer to the displacements formulation of the FEM.

Upon substitution of the previous notations, the incremental Eqn.(4) becomes

$$[K_t]\{\Delta q\} = \{\varphi_{res}\} + \Delta\lambda\{f\} \tag{6}$$

Since the load level λ is treated as a variable, an extra governing equation is required and this is given by a constraint relationship of the form $c(\{\Delta q\}, \Delta\lambda)$. Finally the following complete system follows

$$\begin{cases} [K_t]\{\Delta q\} &= \Delta\lambda\{f\} + \{\varphi_{res}\} \\ c(\{\Delta q\}, \Delta\lambda) &= 0 \end{cases} \tag{7}$$

The constraint equation is method dependent. In the numerical applications we will refer to a modified version of the arc-length method as proposed in [17] and [23] in conjunction with full Newton-Raphson method.

2.3 Description of the plate elements

The contents of this section should be considered a brief description of the detailed formulation quoted in the author's work [17],[18] and [20], in which explicit expression of vectors and matrixes are quoted.

Displacement model. In order to take into account the effects of the transverse shear deformation, the displacements field is assumed to be of the following Reissner-Mindlin form

$$\begin{aligned} u(x,y,z) &= u^o(x,y) + z\phi_x(x,y) \\ v(x,y,z) &= v^o(x,y) + z\phi_y(x,y) \\ w(x,y,z) &= w^o(x,y) \end{aligned} \tag{8}$$

in which x, y and z denote the coordinates of an orthogonal cartesian reference system, see also Fig.1. u, v and w denote the displacements of a generic point along the directions x, y and z respectively. u^o, v^o and w^o are the displacement components of a point on the reference surface Ω of the plate. ϕ_x and ϕ_y denote the rotations of the normal to the reference surface in the planes $x-z$ and $y-z$ respectively, in which the rotations due both to the bending deflections $(w_{,x}, w_{,y})$ and to the shear deformations are included.

The displacement field (8) permits us to refer to isoparametric formulation. According to isoparametric formulations the unknown functions in the domain Ω of the element can be written as the coordinates

$$(u^o, v^o, w^o, \phi_x, \phi_y) = \{N\}^T\{q\} \tag{9}$$

{N} denotes the vector of N_n components (N_n is the number of the nodes while the apexes T denotes transposition) which are the shape functions.

Hook's law of the lamina. We consider a multilayered plate of constant thickness h, consisting of a finite number N_s of thin layers of orthotropic material and uniform thickness perfectly bonded together. The principal axes of elasticity of any individual layer are assumed

to be parallel with the laminate axes. The material properties and the thickness of each layer may be entirely different. As usual by neglecting the normal stresses σ_{zz} the constitutive relations for any individual layer in matrix form hold:

$$\{\sigma_s\} = [Q_s]\{\epsilon_s\} \tag{10}$$

Strain-displacement relations. In a cartesian triorthogonal reference system, the following nonlinear strain- displacement relations of von Kármán type hold

$$\epsilon_{xx} = u_{,x} + \frac{1}{2}w_{,x}^2 ; \quad \epsilon_{yy} = v_{,y} + \frac{1}{2}w_{,y}^2$$

$$\epsilon_{xy} = u_{,y} + v_{,x} + w_{,x}\,w_{,y} \tag{11}$$

$$\epsilon_{xz} = u_{,z} + w_{,x} ; \quad \epsilon_{xz} = v_{,z} + w_{,y}$$

Upon substitution of the Eqns.(8) and (9) in the previous ones, the following relations in matrix form hold

$$\{\epsilon\} = \{\epsilon_l\} + \{\epsilon_{nl}\} = [B]\{q\} = ([B_l] + [B_{nl}])\{q\} \tag{12}$$

$[B_l]$ and $[B_{nl}]$ denote the displacement independent and dependent part of the matrix $[B]$ respectively. The strain variations are:

$$\delta\{\epsilon\} = [B^d]\delta\{q\} ; \qquad [B^d] = [B_l^d] + [B_{nl}^d] \tag{13}$$

where

$$[B_l^d] = [B_l] ; \qquad [B_{nl}^d] = 2[B_{nl}] \tag{14}$$

Secant stiffness matrix $[K_S]$. Within our assumptions, the secant stiffness matrix can be computed by writing the variation of the elastic strain energy as in the following

$$\delta\Psi = <\{\sigma\}^T\{\epsilon\}> = \{q\}^T[K_S]\delta\{q\} \tag{15}$$

and for our elements we have

$$[K_S] = [K_o] + [K_{lnl}] + [K_{nll}] + [K_{nlnl}] \tag{16}$$

where[2]

$$[K_o] = \ <[B_l]^T[Q_s][B_l]> \tag{17}$$

$$[K_{lnl}] = \ <[B_l]^T[Q_s][B_{nl}^d]> \tag{18}$$

$$[K_{nll}] = \ <[B_{nl}]^T[Q_s][B_l]> \tag{19}$$

$$[K_{nlnl}] = \ <[B_{nl}]^T[Q_s][B_{nl}^d]> \tag{20}$$

and

$[K_o]$ is the displacement independent part of $[K_S]$, i.e. the stiffness matrix of the linear problems;

$[K_{lnl}], [K_{nll}], [K_{nlnl}]$ denote the displacement dependent components of $[K_S]$.

[2]In the previous relations we used the notation $< (..) >= \sum_{s=1}^{N_s} \int_{V_s}(..)dV$, in which V_s denotes the volume related to the s-layer.

The derived form of $[K_S]$ is not symmetric. Its symmetrization was proposed in [17]:

$$[K_S] = [K_o] + \frac{1}{2}[K_{nl}] + \frac{1}{2}[K_{\sigma_l}] \tag{21}$$

where $[K_{\sigma_l}]$ has the same structure of $[K_\sigma]$ (see next subsection) but it is only related to the linear part of the stresses in the element.

Tangent stiffness matrix $[K_T]$. Within our assumptions, the tangent stiffness matrix can be computed by writing the second variation of the elastic strain energy in the following way

$$\delta^2\Psi = \delta(\delta\Psi) = \delta\{q\}^T[K_T]\delta\{q\} \tag{22}$$

After same manipulations we get the following form:

$$[K_T] = [K_o] + [K_{nl}] + [K_\sigma] \tag{23}$$

where

$$\delta\{q\}^T[K_\sigma] = <\{\sigma\}^T\delta[B^d]> \tag{24}$$

$$[K_{nl}] = [K_{lnl}] + 2[K_{nll}] + 2[K_{nlnl}] \tag{25}$$

in which

$[K_o]$ is the displacement independent part of $[K_T]$, it's the same as that in $[K_S]$;

$[K_{nl}]$ denotes the nonlinear contribution directly displacement dependent, it is the same at Eqn.(22);

$[K_\sigma]$ denotes the nonlinear contribution coming from terms which appear in the form of stress resultants times curvatures. It is known as initial stress stiffness matrix or geometric stiffness matrix.
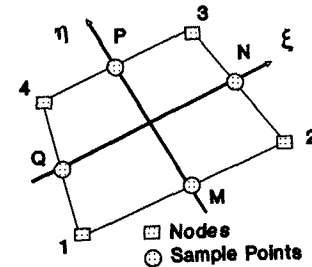

Figure 2: Nodes and sample points in the Q4 finite element.

Assumed shear strain concept. Because of its low band length, in this subheading we refer to particular case of the Q4 finite element. Large literaure has shown that numerical tricks as reduce or selective integration of the stiffness matrix are not sufficient to improve the performances of Q4 element. Patch tests have revealed that in large displacements analyses while

reduce integration often causes zero determinat of these matrixes, the selective case could lead to solutions oscillating around the equilibrium paths. In order to establish numerical efficiency, the assumed shear strain concept was applied in [20] to the multilayered plate formulation above presented. Based on a mixed interpolation of the tensorial components the method differently treats the shear contribution to the stiffness matrix in respect to those coming from the bending and in plane parts deformations. The shear stiffness is not computed at the nodes but in correspondence to four sample points M, N, P and Q (see Fig.2) according to the following interpolations of the shear strain fields:

$$\epsilon_{xz} = \frac{1}{2}(1 + \eta)\epsilon_{xz}^P + \frac{1}{2}(1 - \eta)\epsilon_{xz}^M \qquad (26)$$

$$\epsilon_{yz} = \frac{1}{2}(1 + \xi)\epsilon_{yz}^Q + \frac{1}{2}(1 - \xi)\epsilon_{yz}^N \qquad (27)$$

In which ξ, η denote the natural coordinate on Ω. The theoretical fundamentals of such approximation in relation to mixed concepts are discussed in many published papers, see Hinton and Huang [16] for example.

Laminates and mechanical datas	
LAM1	$(0°/90°/45°/-45°)_{symm.}$
LAM2	$(0°/90°)_{symm.}$
LAM3	$(0°/90°/45°/-45°)_2$
Mech1	$E_l = 40, E_t = 1, G_{lt} = G_{tt} = .5, \nu = .25$
Mech2	$E_l = 40, E_t = 1, G_{lt} = .5, G_{tt} = .2, \nu = .25$
Description of geometrical boundary conditions	
SSSS	$x = 0, b \rightsquigarrow w = 0; \ y = 0, b \rightsquigarrow w = 0$
HSSS	$y = 0 \rightsquigarrow u = v = w = 0; \ y = b \rightsquigarrow w = 0;$
	$x = 0, b \rightsquigarrow w = 0$
CCCC	$x = 0, b \rightsquigarrow w = \phi_{yz} = 0;$
	$y = 0, b \rightsquigarrow w = \phi_{xz} = 0$
Tab 1. Datas for the introduced acronyms.	

3 Results and discussion

Tab.1 gives the mechanical properties of the utilized laminae and the introduced notations to indicate boundary conditions. The standard symbols have been used to denote mechanical properties of the lamina along the orthotropic directions l and t. We refer to consistent unit in all the investigations. Three laminates are considered, two of these are symmetric (one of which is ortotropic), the third one is not symmetric. Two simply supported and one clamped geometrical boundary conditions are taken into account.

Exception made of Fig.5 where the nine node element Q9 of lagrangian family has been used, the Q4 element with assumed shear strain fields will be employed. Imperfections will be simulated by application of transverse disturb loads in the form of a point load P_{dis}^{z*} (applied at the plate center) or a constant distribution of pressure p_{dis}^{z*}. With reference made to Fig.1,

the in plane applied loads are denoted by N_{xx}, N_{yy} and N_{xy}, i.e. compression along the directions x and y, and shear load respectively. These values correspond to the resultant forces which are uniformly distribuited at nodes along the edges of the plate. The apex '*' denotes components of the reference load vector $\{f\}$ so that, according to Eqn.(3), effective loads hold:

$$P_{dis}^z = \lambda P_{dis}^{z*}; \quad p_{dis}^z = \lambda p_{dis}^{z*}.$$

Likewise the in-plane loads are:

$$N_{xx} = \lambda N_{xx}^*; \quad N_{yy} = \lambda N_{yy}^* \quad and \quad N_{xy} = \lambda N_{xy}^*.$$

$a, b,$ and h are the geometric plate dimensions along the x, y and z directions respectively. The FSDT and CLT results are referred to the value $\chi = 5/6$ and $\chi = 10$ respectively. All the results takes the form of laod parameter λ vs transverse displacement at the plate center W_c. We make note that W_c is not always coinciding to the maximum normal deflection of the plates. This depends on the laminate and both mechanical and geometrical boundary conditions. Additional datas of the treated problems are directly quoted in captions and sketches of the figures.
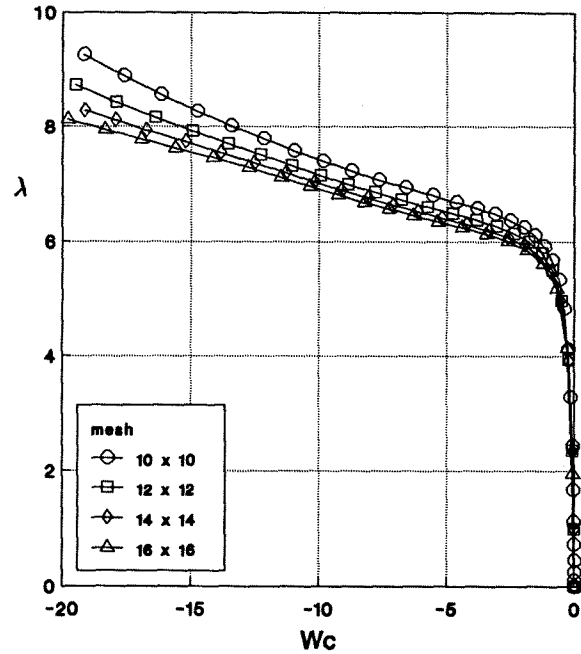

Figure 3: Convergence analysis of Q4 finite element with assumed shear strain fields, for a square compressed plates. Datas: $N_{yy}^* = -33$, $p_{dis}^{z*} = -3.E-5$; $a=b=100$, $h=10$; LAM2, Mech2; SSSS.

Fig.3 shows the convergence rate of the Q4 element. Different meshes are considered: from 10x10 (100 elements) to 16x16 (256 elements). The nonlinear response in both prebuckling and postbuckling range of a

square compressed thick simply supported plate is analysed by means FSDT. A symmetric lamination scheme is investigated and the transverse disturb has the form of a constant distribution of normal pressure.
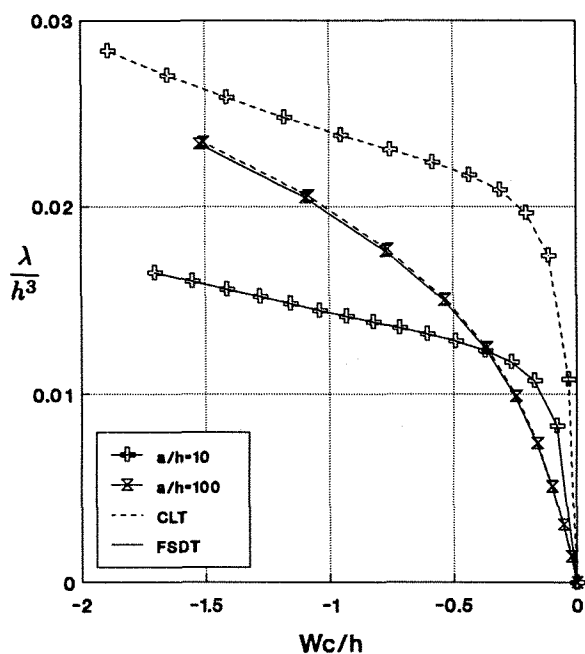

Figure 4: Effect of shear deformation vs plate thickness for square compressed plates. Datas: $N_{yy}^*=-13$, $P_{dis}^{*z}=-.1$; a=b=120; mesh 12x12, Q4; LAM2, Mech2; SSSS.

Effects of thickness and ortotropic ratio on postbuckling of compressed plates.

To highlight the effects of transverse shear deformations Fig.4 compares a thick orthotropic compressed plate plate to a thin one. For scale reason the value $\frac{\lambda}{h^3}$ is plotted at the y-axis. Fig.5 compares two compressed plates related to two different values of the ortotropic ratio $\frac{E_l}{E_t}$. Then we confirm that thickness and orthotropic ratio increasing, the transverse shear effects cannot be neglected. Moreover the importance of this effects increase in the large deflections field.

Postbuckling of in-plane loaded symmetrically laminated plates.

Figs.6-9 compare the postbuckling response of two symmetrically laminated plates. Both CLT and FSDT results are plotted and four different loading cases are considered: axial compression, biaxial compression, shear and combined. Imperfection has been simulated by application a transverse disturb load at the plate center. Value of the W_c double of the plate thickness h are investigated. W_c increasing the equilibrium state depends on both lamination scheme and loading case. In particular the shear deformation effects assume more importance for the in-plane shear loading cases.
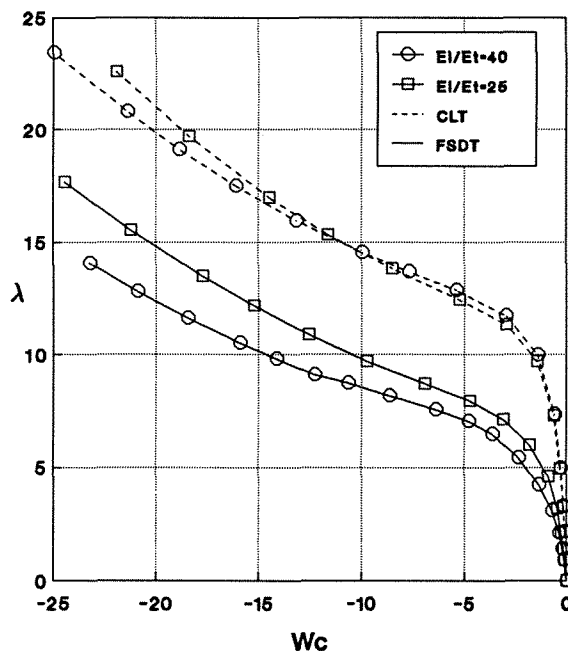

Figure 5: Effect of shear deformation vs ortotropic ratio $\frac{E_l}{E_t}$ for square compressed plates. Datas: $N_{yy}^*=-20$, $p_{dis}^{*z}=-.2$; a=b=9, h=10; mesh 4x4, Q9; LAM2, Mech2 with variable E_l; HSSS.
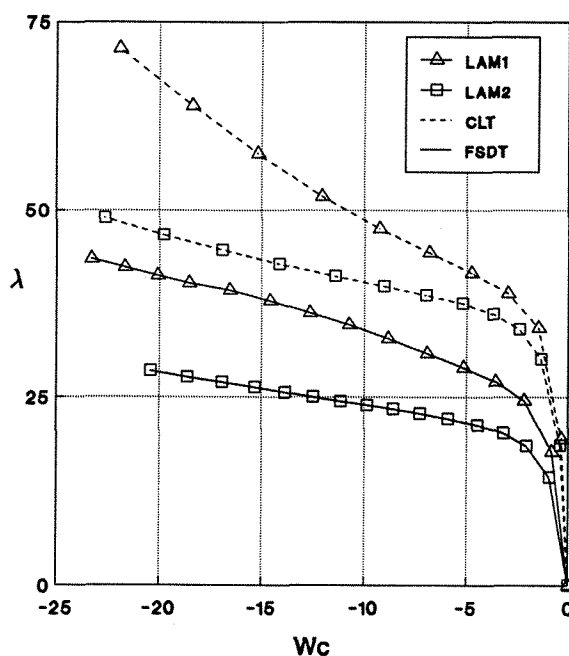

Figure 6: Comparison of two symmetric laminates for a square axially compressed plate. Datas: $N_{yy}^*=-13$, $P_{dis}^{*z}=-.1$; a=b=120, h=12; mesh 12x12, Q4; LAM1 with Mech1, LAM2 with Mech2; SSSS.
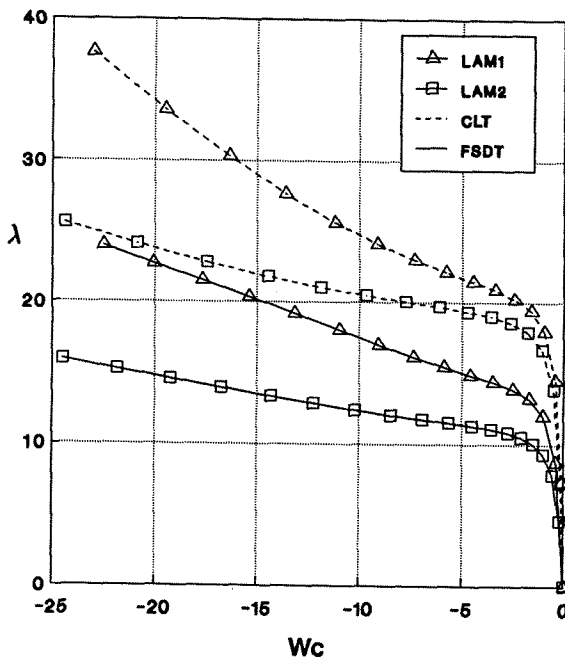
Figure 7: Comparison of two symmetric laminates for a square biaxially compressed plate. Datas: $N_{yy}^* = N_{xx}$=-13, P_{dis}^{*z}=-.1; a=b=120, h=12; mesh 12x12, Q4; LAM1 with Mech1, LAM2 with Mech2; SSSS.
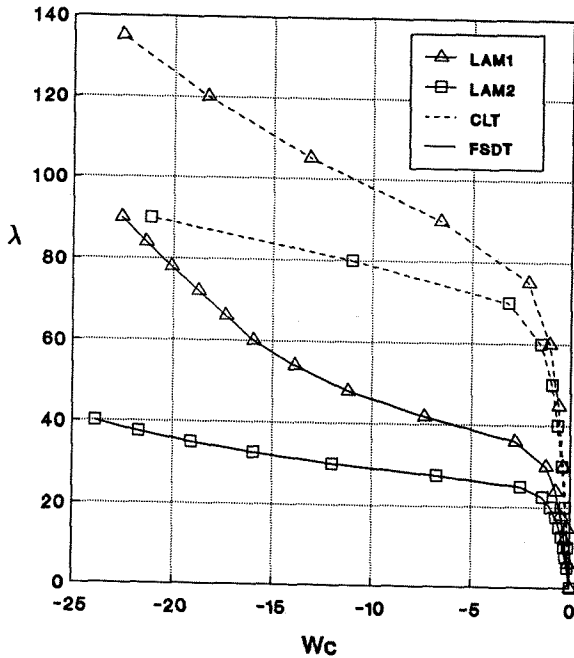

Figure 8: Comparison of two symmetric laminates for a square plate subjected to in-plane shear loading. Datas: N_{xy}^*=-13, P_{dis}^{*z}=-.1; a=b=120, h=12; mesh 12x12, Q4; LAM1 with Mech1, LAM2 with Mech2; SSSS.

Postbuckling of in-plane loaded not symmetrically laminated plates. Not symmetrically laminated plates are considered in Figs.10-11.

Because of the coupling stiffnesses B_{ij} (between in-plane and out-of-plane deformations), no disturb loads need to create initial inflections. Fig.10 compares three loading cases: compression, shear and combined. As for the symmetrically laminated plates, the shear deformation effects are very much affected by loading cases.

By variyng the ortotropic ratio Fig.11 considers the effect of the coupling stiffness on the postbuckling of shear loaded plates. We notice that the shear deformation effects very much depend on coupling stiffnesses magnitude.
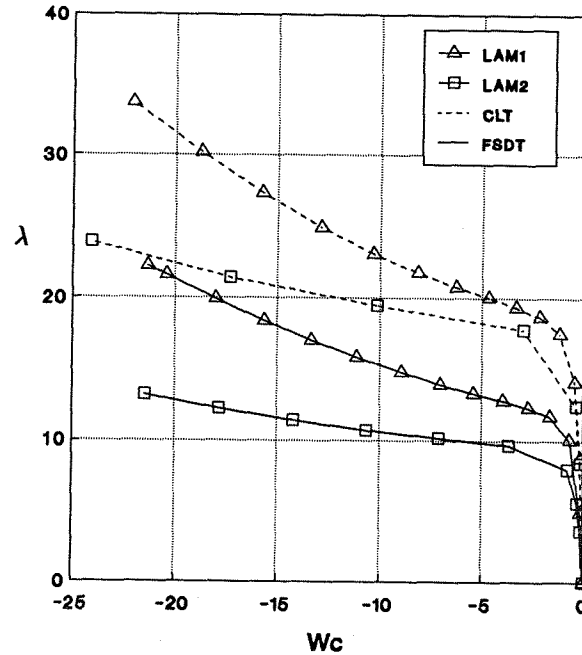

Figure 9: Comparison of two symmetric laminates for a square plate subjected to combined loads: shear and biaxial compression. Datas: $N_{yy}^* = N_{xy}^* = N_{xy}^*$=-13, P_{dis}^{*z}=-.1; a=b=120, h=12; mesh 12x12, Q4; LAM1 with Mech1, LAM2 with Mech2; SSSS.

Comparison of two possible manners of loading plate edges. In the linear analysis or in the buckling of plates (classical bifurcation analysis of Euler-type), the distribution of the load along the plate edges which leads to a constant distribution of the correspondent in-plane displacements is assumed load level independent. In fact in the classical eigenvalues analysis this ditributions increase by means of a loads factor until a bifurcation point has been reached. In the analysis at the previous figures we have done the same, in fact in our FEM formulation the loads increase throught the load parameter λ.
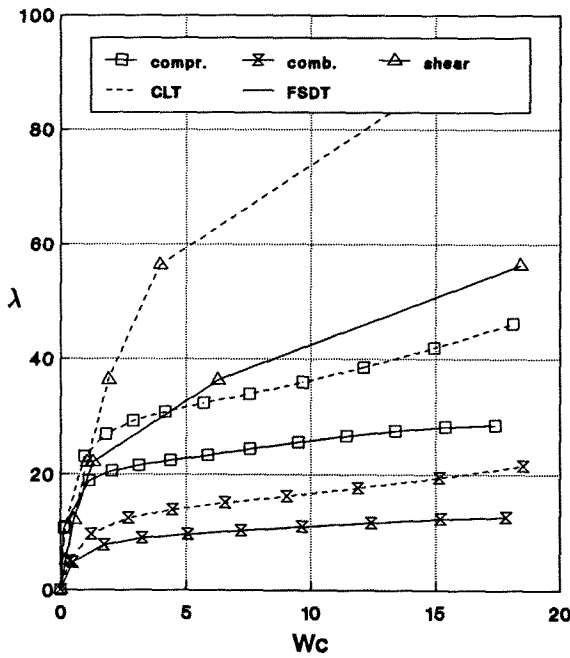
2970

Figure 10: Comparison among three different loading cases for a square not symmetrically laminated plates. Datas: $compr$ $N_{yy}^*=-13$, $comb$ $N_{yy}^* = N_{xy}^* = N_{xy}^* =-13$, $shear$ $N_{xy}^*=- 13$; a=b=120, h=12; mesh 12x12, Q4; LAM3, Mech1; SSSS.

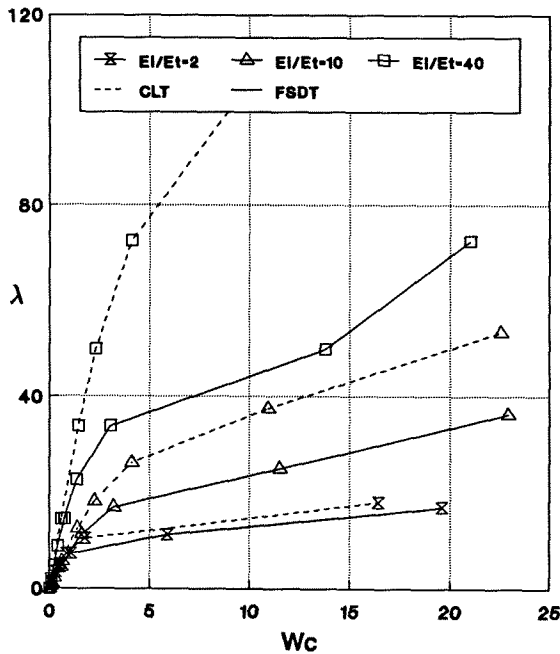
Figure 11: Effect of coupling stiffnesses B_{ij} for a square not symmetrically laminated plates subjected to shear loadings. Datas: $N_{xy}^*=- 13$; a=b=120, h=12; mesh 12x12, Q4; LAM3, Mech1; SSSS.

But in the large deflections range, as revelead in [7] and [18], the load ditributions which need to maintain the relative edge displacements distribution constant is load level dependent. In Fig.12 the two possibilities of uniform loads and uniform diplacements distribution at the loaded edges are compared in the case of axial compressed clamped plate. To do this two rows of stiff Q4 plate elements (which have E_l values four order of magnitude stiffer than E_l of the plate) are added to the initial FEM mesh in correspondence of the loading edges $y = 0, b$. This FEM model enforces to be constant the distribution of the displacements along the loaded edges. To notice that N_{xx} resultant value is preserved. Fig.12 shows that the two FEM models have a very good agreement in the small deflection fields. In fact the buckling load prediction is quite the same for both CLT and FSDT cases. But deflections increasing the differences tragically grow up. Even thought we have not plotted the deformations modes, we have checked that they are the same for the two cases. It is not obvious to estabilish which one of the two extreme investigated simulations is the most realistic, very probabily the right one is in between. But we can certainly conclude that in non linear field much more care must be given to the manners in which boundary conditions are simulated.

Change path phenomenon for a rectangular plate

biaxially compressed. Equilibrium related to the rectangular biaxially compressed plate are quoted at Fig.13. A transverse constant distribution of pressure has been applied as disturb load. Two value of the ortotropic ratio are considered. The geometry and boundary conditions are drawn at Fig.14. Two rows and two columns of Q4 stiff finite elements have been introduced as at the Fig.12 analysis; these Q4 elements have the aims to simulate usual stiffners and to impose constant in-plane displacements at the edges. The plate is simply supported along the boundaries denoted by a circle at Fig.14. We notice that because of the stiffners the rotations at the edges are constrained to be very small. That is the plate in reality is not simply supported. The two traced equilibrium paths reveal that the plate center W_c changes its sign. That happens in correspondence to very small value of W_c and it very much depends on the ortotropic ratio value. For some equilibrium points Fig.15 quotes the deformation modes correspondento to those depected at Fig.13. At low load level the modes are mainly constrained by the normal pressure, but load increasing higher modes are stabilyzed. We notice that this phenomen has already been found and explained by Carrera and Villani [7] and it is related to the FEM arc-lenth-type method used at Eqns.(7).
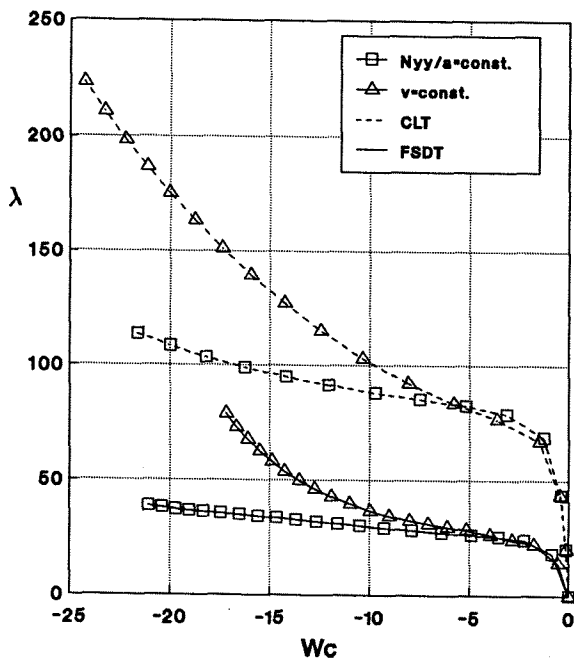
2971

Figure 12: Comparison of two different manners of imposing boundary conditions for a square symmetrically laminated plates subjected to axial compression. Datas: $N^*_{xy}=-13$, $P^{*z}_{dis}=-.1$; a=b=120, h=12; mesh 12x12, Q4; LAM2, Mech2; CCCC.
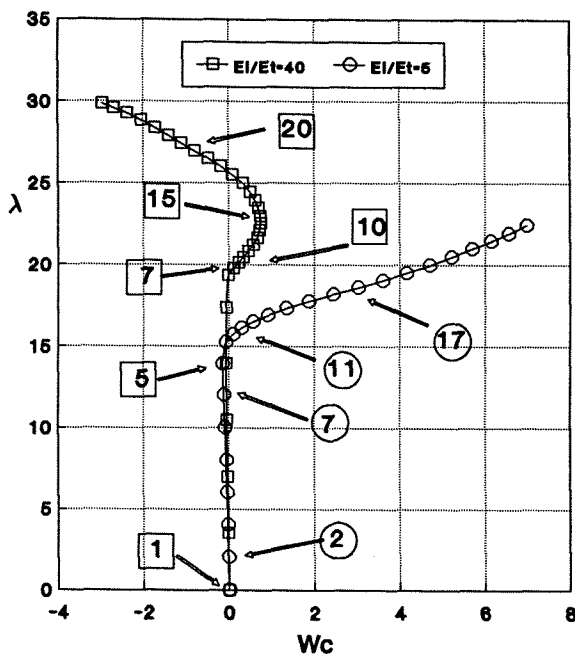

Figure 13: Effect of ortotropic ratio and change path phenomenon for a rectangular laminated plates biaxially compressed. Datas: $N^*_{yy}=-9$, $N^*_{xx}=-20$, $p^{*z}_{dis}=-1.E-5$; a=80,b=260, h=10; mesh 8x26, Q4; LAM2, Mech2; CCCC.
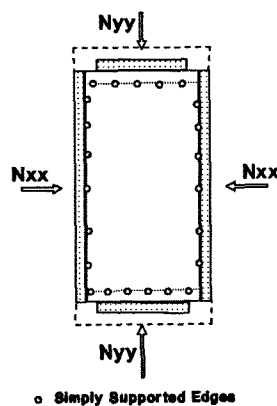

Figure 14: Description of boundary conditions used for long plates analysis at Fig.13.

Concluding remarks

The paper has applied a FEM model to analyse the nonlinear response of generally laminated flat panels subjected to several geometrical and mechanical boundary conditions. This model takes into account the shear deformation effects and furnishes as a particular case results related to the Kirchhoff approximations. In order to preserve computation time the numerical investigations have been carried out by the use a four node finite element with assumed shear strain fields. From these analyses we remark what follows:

1. The FEM is a good tool to trace the postbuckling of anisotropic flat panels. Further in respect to other approximate methods, its possible application does not depend on both boundary conditions and lamination schemes. It fact it has been applied to several in-plane loading conditions, different geometrical boundary conditions, symmetrically and not symmetrically laminated plates.

2. It is confirmed that the nonlinear effects are very important in the analysis of multilayered plates and that the shear deformation effects are very much subordinate to both multilayered lay-up and loading configurations, furthermore they are greater in the large deflections field.

3. Much more care should be taken to impose boundary conditions in the postbuckling range. In fact by comparing results relate to constant distributions of the displacements at the edges to those coming from a constant distribution of the applied loads at the same edges, we have found that while the prebuckling and buckling states are quite close in the two cases, the postbuckling equilibrium state can be very different.

2972

4. The changes of buckled paths, typical of experimental tests, have been observed for a long plate biaxially compressed and in correspondence to low values of the transverse displacements.
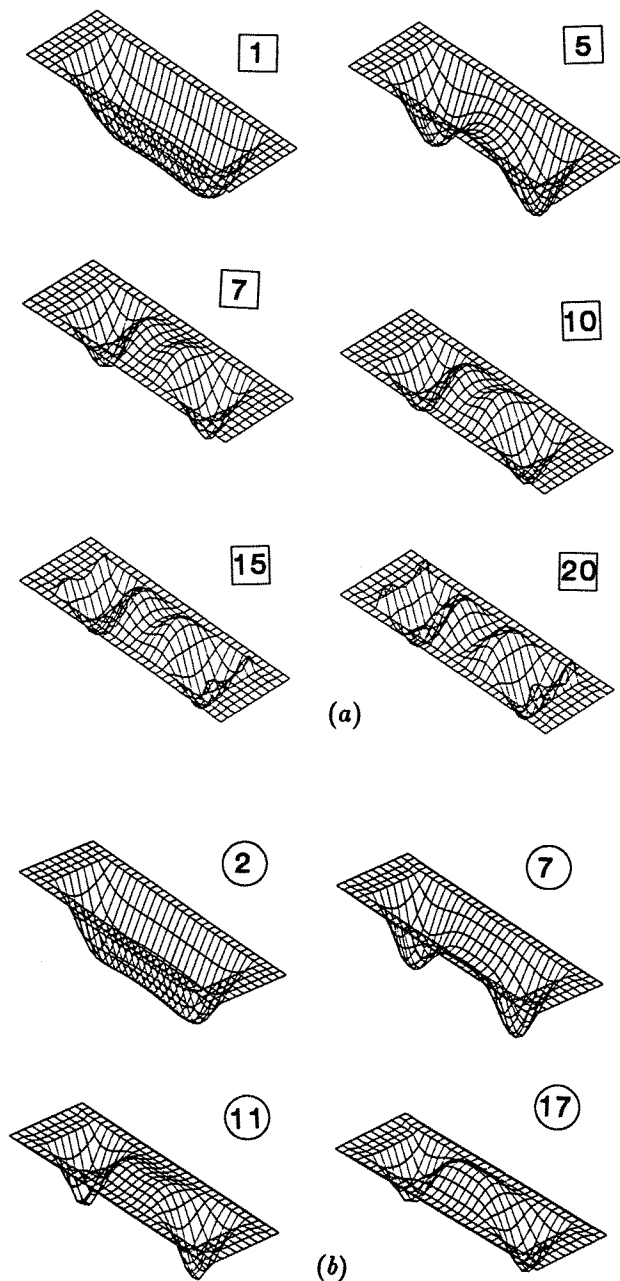

Figure 15: Shapes related to equilibrium paths depicted at Fig.13: (a) $\frac{El}{E_t} = 40$; (b) $\frac{El}{E_t} = 5$.

Additional investigations need to compare the several geometrical and mechanical boundary conditions as well as plate geometries and lamination schemes. Particular attention should be given to the manner in which the loads are applied. Moreover to accurately predict the stress-strain fields in the nonlinear range HSDT effects should be included in the formulations. These could be subjects for future works.

References

[1] Chai C B, Banks W M, Rhodes J, *An experimental studies on laminated panels in compression*, Composite Structures, Vol 19, pp 67-87, 1991

[2] Noor A K, Burton W S, *Assestement of shear deformation theories for multilayered composite plates*, Applied Mechanics Review, Vol 42, pp 1-13, 1989

[3] Librescu L, Stein M, *Postbuckling behaviour of shear deformable composite flat panels taking into account geometric imperfections*, American Institute of Aeronautics and Astronautics Journal, Vol 30, pp 1352-1360, 1992

[4] Librescu L, Chang M Y, *Imperfections sensitivity and postbuckling behaviour of shear deformable composite doubly curved shallow panels*, International Journal of Solids and Structures, Vol 29, pp 1065-1083, 1992

[5] Librescu L, Chang M Y, *Effects of geometric imperfection on vibration of compressed shear deformable laminated composite curved panels*, Acta Mechanica, Vol 96, pp 203-224, 1993

[6] Palazotto A N, Tsai C T, *A Modified Riks approach to composite shell snapping using a high-order shear deformation theory*, Computers & Structures, Vol 35, pp 221-226, 1990

[7] Carrera E, Villani M, *Large deflections and stability FEM analysis of shear deformable compressed anisotropic flat panels*, submitted for pubblication

[8] Sun C T, Chin H, *Analysis of asymmetric composite laminates*, American Institute of Aeronautics and Astronautics Journal, Vol 26, pp 714-718, 1988

[9] Jensen D W, Lagace P A, *Influence of mechanical couplings on the buckling and postbuckling of anisotropic plates*, American Institute of Aeronautics and Astronautics Journal, Vol 26, pp 1269-1277, 1988

[10] Leissa A W, *Conditions for laminated plates to remain flat under in-plane loading*, Composite Structures, Vol 6, pp 261-270, 1986

[11] Carrera E, *On the non linear response of asymmetrically laminated plates in cylindrical bending*, American Institute of Aeronautics and Astronautics Journal, Vol 31, pp 1353-1357, 1993

[12] Chia C Y, Nonlinear analysis of anisotropic plates, McGraw Hill, New York, 1980

[13] Chia C Y, *Geometrically nonlinear behaviour of composite plates: a review*, Applied Mechanics Review, Vol 41, pp 439-450, 1988

[14] Crisfield M A, Non-linear finite element analysis of solids and structures, John Wiley, London, 1992

[15] Palazotto A N, Dennis S T, Nonlinear analysis of shell structures, AIAA Series, 1992

[16] Hinton E, Huang H C, *A family of quadrilater mindlin plate elemnets with substitute shear strain fields*, Computer & Structures, Vol 23, pp 409-431, 1986

[17] Carrera E, *Large deflection behaviour and incremental strategies in the FEM analysis of composite structures*, ISD Report 10/92, University of Stuttgart, 1992

[18] Carrera E, *Postbuckling behaviour of multilayered shells* (in Italian), Ph.D Thesis, DIAS, Politecnico di Torino, Torino, 1991

[19] Dvorkin E N, Bathe K J, *A continuum mechanics based four-node shell element for general non linear analysis*, Engng. Comput, Vol 1, pp 77-88, 1984

[20] Carrera E, *On a simple finite plate element computationally efficient and able to include HSDT effects*, to appear in Aerotecnica Missili e Spazio,

[21] Washizu K, Variational methods in elasticity and plasticity, Pergamon Press, N Y, 1968

[22] Zienkiewicz O, Finite element method, fourth editions, Mc Graw Hill, London, 1990

[23] Carrera E, *A study on arc-length-type methods and their operation failures illustrated by a simple model*, Computer & Structures, Vol 50, pp 217-229, 1994